ISSN 1063-7761, Journal of Experimental and Theoretical Physics, 2006, Vol. 102, No. 6, pp. 972–985. © Pleiades Publishing, Inc., 2006.
Original Russian Text © V.A. Gavrichkov, S.G. Ovchinnikov, L.E. Yakimov, 2006, published in Zhurnal Éksperimental'noĭ i Teoreticheskoĭ Fiziki, 2006, Vol. 129, No. 6, pp. 1103–1117.

ELECTRONIC PROPERTIES OF SOLIDS

The Role of Orbital Ordering in the Formation of Electron Structure in Undoped $LaMnO_3$ Manganites in the Regime of Strong Electron Correlations

V. A. Gavrichkov[a],*, S. G. Ovchinnikov[a], and L. E. Yakimov[b]

[a] *Kirensky Institute of Physics, Siberian Division, Russian Academy of Sciences, Krasnoyarsk, 660036 Russia*
[b] *Siberian State Aerospace University, Krasnoyarsk, 660014 Russia*
**e-mail: gav@iph.krasn.ru*

Received September 30, 2005

Abstract—The electron structure of undoped $LaMnO_3$ and slightly doped $La_{1-x}Sr_xMnO_3$ manganites has been calculated within the framework of a generalized tight binding method with explicit allowance for strong intraatomic electron correlations. According to the results of these calculations, the ground state in orbitally disordered undoped $LaMnO_3$ ferromagnets would be metallic despite the Mott–Hubbard correlation gap in the spectrum of quasiparticles. Owing to the orbital ordering, the insulating state is stabilized in both antiferromagnetic and paramagnetic phases. In-gap states of a polaron nature with a spectral weight proportional to the dopant concentration have been found near the top of the valence band in $La_{1-x}Sr_xMnO_3$. As the doping level increases, a metal state appears in the ferromagnetic phase, which has a metallic character for one spin subband and an insulating character for the other subband (representing the so-called half-metallic state).

PACS numbers: 71.10.–w

DOI: 10.1134/S1063776106060112

1. INTRODUCTION

A starting point in most discussions concerning the mechanisms of magnetoresistance, metal–insulator transition, and ferromagnet–paramagnet (FM–PM) transition in manganites is the model of double exchange [1]. According to Anderson and Hasegawa [2] and de Gennes [3], the physics of double exchange consists in the hopping amplitude t depending on the spin configuration in two nearest neighbor sites. The double exchange model provides an intuitively clear explanation both for the interrelation of spin and charge degrees of freedom and for the mobility of carriers. The main problem consists in the fact that this model cannot quantitatively describe the magnitude of the conductivity change upon the metal–insulator transition [4]. Indeed, in a PM state ($T > T_C$), the angle between two adjacent spins is 90° and, hence, the amplitude of the hopping integral t_{eff} decreases by a factor of $\cos(90°/2) = 0.7$ as compared to the value in the FM state, which implies the same decrease in the conductivity. However, as is well known, a decrease in the conductivity upon the FM $\longleftrightarrow$ PM transition in experiment reaches 2–3 orders of magnitude. The discrepancy reaching orders of magnitude indicates that some other factors are responsible for a change in the conductivity observed upon the FM $\longleftrightarrow$ PM transition. Another conclusion is that the quasiparticle band width also decreases by a factor of 0.7 relative to the value in the FM state. This implies a small increase in the density of states at the Fermi level (E_F) in the PM phase. This conclusion also contradicts experimental facts that give evidence for the formation of a pseudogap at E_F when the temperature increases above T_C. Indeed, the conductivity is determined by the density n and mobility μ of charge carriers (electrons) as $\sigma = ne\mu$. In the double exchange model, a change in the carrier mobility is the predominant factor, since it is related to the corresponding change in the amplitude of the hopping integral. An additional decrease in the mobility can be related to the influence of Anderson localization (e.g., to a disorder in the arrangement of spins of t_{2g} electrons). However, neither of these factors has any significant influence on the density of states at E_F. Experimental data on the Hall effect [5] and the angle-resolved photoemission [6] clearly indicate that the metal–insulator transition takes place due to a change in the density of carriers (i.e., in the density of states at E_F), rather than in the mobility. This discrepancy between the conclusions following from experiment and the double exchange model cannot be considered quantitative alone.

Another direction of research is related to ab initio calculations of the electron spectrum of manganites as dependent on the type of magnetic and orbital ordering, doping level, and distortions of the crystal structure. A distinctive feature of these calculations is a realistic approach to the band structure of manganites. However, the applicability of the one-electron approach to calcu-

lations of the band structure of $LaMnO_3$ is disputable. Indeed, in accordance with estimates [7], the magnitude of the single-site Coulomb interaction U is about 8 eV in both $LaMnO_3$ and $SrMnO_3$, while the energy of charge pd fluctuations is $\Delta = 4.5$ eV for $LaMnO_3$ and 2 eV for $SrMnO_3$. According to the scheme of Zaanen–Sawatzky–Allen [8], these compounds should be classified as charge-transfer insulators in which electron correlations form the insulating ground state. In fact, one-electron calculations within the framework of the density functional theory (LSDA DFT) [9] stipulate a metallic state for the cubic structure in accordance with the partly filled d band. An analogous result is obtained for undoped cuprates of the La_2CuO_4 type [10].

A permanent disadvantage of the one-electron calculations (LSDA, LDA+U) is also related to the fact that a giant exchange splitting of quasiparticle states with respect to spin (~3 eV for t_{2g} states of manganese) is introduced in order to explain the formation of a larger magnetic moment in FM and antiferromagnet (AFM) phases. This leads to some incorrect conclusions concerning AFM and PM phases. For example, it was stated [9] that the spectra of quasiparticles with various spin projections in AFM differ from each other. This is a rather strange result, since the AFM background is identical for the charge carriers with various spin projections. For the PM phase, no exchange gap is present in the spectrum of quasiparticles, and both the spin-polarized model and LDA calculations lead to the metallic state.

In searching for answers to the aforementioned challenges, we have studied the band structure of manganites using a substantially modified, generalized tight binding method which was previously developed for layered cuprates [11]. Since the differences in the physics of manganites and cuprates are obviously very substantial, it is clear that they cannot be reproduced by merely changing parameters of the basic method. In addition to two differences of purely technical character, which are related to a three-dimensional nature of the cubic crystal structure of $LaMnO_3$ and to high-spin many-electron terms of the d^5, d^4, and d^3 configurations of manganese, there is another important difference related to the orbital ordering in manganites. As a result, manganites feature the coexistence of various magnetically and orbitally ordered states [12], this situation having no analog in cuprates.

In order to develop a generalized tight binding method for the calculation of a quasiparticle spectrum in orbitally ordered $LaMnO_3$, we constructed a two-sublattice configuration space on high-spin states corresponding to the ground states of a cell with different numbers of electrons. Then, using the method of Hubbard operators acting in the space of high-spin states, we calculated the dispersion for AFM, FM, and PM phases.

The results of our calculations indicate that, despite the Mott–Hubbard correlation gap in the spectrum of quasiparticles, the ground state of undistorted cubic $LaMnO_3$ possessing the AFM order would be metallic merely due to the degeneracy of e_g orbitals (the Hubbard model for $U \longrightarrow \infty$ with 1/4 filling stipulates a metallic state). The existence of Jahn–Teller distortions, which introduce $\Delta\varepsilon$ splitting into the e_g level, leads to the insulating ground state. The orbital ordering in AFM and PM phases results in the subbands of two different types separated by an energy gap on the order of $\Delta\varepsilon$ appearing on top of the valence band. The FM phase exhibits differences between the spectra of quasiparticles with different spin projections. However, this is not a simple shift of spin subbands analogous to that in LSDA calculations. The differences in the FM phase are related to a redistribution of the spectral intensity between the states of carriers with different spin projections. At the same time, the spectra of quasiparticles in AFM and PM phases remain doubly degenerate with respect to spin.

This paper is organized as follows. Section 2 gives formulation of the many-electron model and introduces the Hamiltonian for a two-sublattice state of the orbital antiferromagnetism. Section 3 is devoted to exact diagonalization of the many-electron Hamiltonian in the basis of high-spin configurations: d^5p^6 ($S = 5/2$), $d^4p^6 + d^5p^5$ ($S = 2$), $d^3p^6 + d^4p^5 + d^5p^4$ ($S = 3/2$). In Section 4, the construction of Hubbard operators on this basis is describes and a dispersion equation of the generalized tight binding method for the band structure of quasiparticles is obtained. Section 5 gives an analysis of obtained band structures of the AFM and PM phases of undoped $LaMnO_3$ and the FM and PM phases of doped $La_{1-x}Sr_xMn_xO_3$ manganites with a hole dopant concentration of $x \approx 0.2$–0.3. The final Section 6 contains the main conclusions.

2. FORMULATING THE PROBLEM AND CONSTRUCTING THE HAMILTONIAN

Let us begin with some statements, which we believe to be necessary for the formulation of the problem under study in view of the results of recent investigations into the properties of manganites, since otherwise any theoretical analysis can be unsound. From this standpoint, the construction of an adequate computational scheme for $LaMnO_3$ manganites requires the following:

(i) Making allowance for the orbital ordering (the cooperative Jahn–Teller effect) [12];

(ii) Constructing a configuration space of the electron subsystem on a basis of high-spin states;

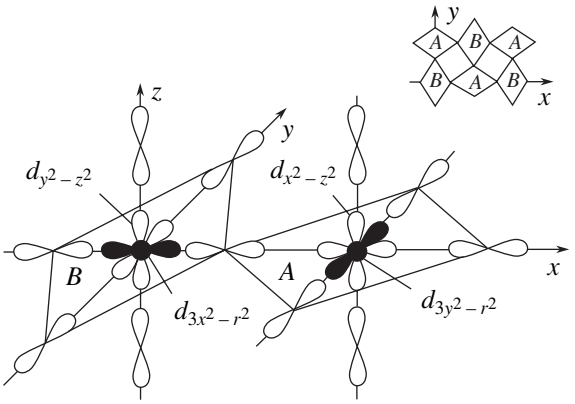

Fig. 1. Subdivision of the spatial structure of $LnMnO_3$ into sublattices A and B according to [12], e_g states of manganese $|\theta\rangle$ in these sublattices, and p states of oxygen involved in $dp\sigma$ bonds. The inset shows a structural motif of the cooperative effect, which corresponds to antiferroorbital ordering. The structure is repeated with translation along the z axis.

(iii) Taking into account the Mn3d–O2p hybridization for a correct description of the splitting of Mn3d states in the field of ligands [13];

(iv) Selecting a particular scheme for the calculation of effects due to strong electron correlations in the spectrum of quasiparticles [14–16].

In most investigations devoted to the correlation effects in the electron structure of manganites [17–21], the role of O2p orbitals consists in the introduction of an effective matrix element t_{eff} of hopping between the states of manganese. Estimates show that the splitting of e_g and t_{2g} levels caused by the crystal field in $LaMnO_3$ does not exceed 0.1 eV [13], Therefore, a necessary information concerning the role of the Mn3d–O2p hybridization in the Jahn–Teller splitting of e_g levels can be obtained only by directly involving O2p orbitals in the calculation scheme. Figure 1 illustrates the choice of a minimum basis set of Mn3d and O2p orbitals, which is necessary for calculation of the spectrum of low-lying excitations. In manganites, the Jahn–Teller effect leads to local distortions of the MnO_6 octahedron, which becomes elongated in the xy plane and contracted in the z direction. The symmetry of the Jahn–Teller distortions is such that they remove the degeneracy of e_g orbitals and favor the filling of one of these orbitals ($d_{3z^2-r^2}$ or $d_{x^2-y^2}$). In $LaMnO_3$, the cooperative Jahn–Teller effect leads to occupation of the linear combinations of these local orbitals and stabilization of the alternating $d_{3x^2-r^2}$ and $d_{3y^2-r^2}$ orbitals as the ground ones. As a result, a $\sqrt{2} \times \sqrt{2}$ superlattice is formed in the xy plane (Fig. 1). This phenomenon is known as the antiferroorbital ordering [12]. Thus, with a view to calculate the spectrum of quasiparticle excitations, we select the set of e_g states in $LnMnO_3$ in the following form:

$$|\theta\rangle = \cos\left(\frac{\theta}{2}\right)|d_{3z^2-r^2}\rangle + \sin\left(\frac{\theta}{2}\right)|d_{x^2-y^2}\rangle,$$

where

$$(1)\ \left|\theta = \frac{\pi}{3}\right\rangle = \sqrt{3}(y^2 - z^2) \equiv |d_y\rangle,$$

$$(2)\ \left|\theta = \frac{2\pi}{3}\right\rangle = (3y^2 - r^2) \equiv |d_{3y}\rangle,$$

$$(3)\ \left|\theta = \frac{4\pi}{3}\right\rangle = (3x^2 - r^2) \equiv |d_{3x}\rangle,$$

$$(4)\ \left|\theta = \frac{5\pi}{3}\right\rangle = \sqrt{3}(x^2 - z^2) \equiv |d_x\rangle.$$

Since the $|d_{3y}\rangle$ and $|d_{3x}\rangle$ states in the neighboring sites differ by the angle $\Delta\theta = 2\pi/3$, this configuration represents the so-called slanted AFM state. The $|d_x\rangle$ and $|d_y\rangle$ states are included into the basis set as the first excited states in sublattices A and B, respectively. In order to describe the presence of a $\sqrt{2} \times \sqrt{2}$ superstructure in the xy plane, we subdivide O2p orbitals (forming the σ bonds) between sublattices so that two p_x orbitals (p_{1x} and p_{2x}) and one p_z belong to sublattice A, and two p_y orbitals (p_{1y} and p_{2y}) and one p_z belong to sublattice B. Of course, the Jahn–Teller distortions split not only e_g, but t_{2g} states as well. However, in contrast to e_g, the t_{2g} states exhibit much weaker hybridization with the O2p states. Indeed, the ratio of the integral of hopping via the $dp\sigma$ and $dp\pi$ bonds is $t_\sigma/t_\pi \sim 2$. As a result of this splitting, the low-energy physics of manganites predominantly involves the e_g states. For this reason, the t_{2g} states will be implicitly taken into account in constructing the many-electron terms (see formulas (8), (9), and (11) below. The splitting of t_{2g} states is probably important for the direct calculation of their spectral intensity. However, from the standpoint of the quasiparticle spectrum in $LaMnO_3$, this splitting changes the energy by at least 1–2 eV in the depth of the valence band due to the difference in $pd(e_g)\sigma$ and $pd(t_{2g})\pi$ bonds.

Before proceeding (according to the second initial condition) to the construction of high-spin 3d multiplets, let us write the Hamiltonian on the selected basis set of atomic orbitals and perform diagonalization of the intracell part. The Hamiltonian of the pd electron subsystem can be written as follows:

$$\hat{H} = \hat{H}_d + \hat{H}_p + \hat{H}_{pp} + \hat{H}_{pd},$$

$$\hat{H}_d = \sum_{\mathbf{r}\lambda\sigma}\left[(\varepsilon_\lambda - \mu)\hat{d}^+_{\lambda\mathbf{r}\sigma}\hat{d}_{\lambda\mathbf{r}\sigma} + \frac{1}{2}U_\lambda\hat{n}^\sigma_{\lambda\mathbf{r}}\hat{n}^{-\sigma}_{\lambda\mathbf{r}}\right.$$

$$+\sum_{\lambda'\sigma'}(-J_d\hat{d}^+_{\lambda\mathbf{r}\sigma}\hat{d}_{\lambda\mathbf{r}\sigma'}\hat{d}^+_{\lambda'\mathbf{r}\sigma'}\hat{d}_{\lambda'\mathbf{r}\sigma}+V_{\lambda\lambda'}\hat{n}^\sigma_{\lambda\mathbf{r}}\hat{n}^{\sigma'}_{\lambda'\mathbf{r}})\Bigg],$$

$$\hat{H}_p=\sum_{\alpha\sigma}\Bigg[(\varepsilon_\alpha-\mu)\hat{p}^+_{\alpha\mathbf{i}\sigma}\hat{p}_{\alpha\mathbf{i}\sigma}+\frac{1}{2}U_\alpha\hat{n}^\sigma_{\alpha\mathbf{i}}\hat{n}^{-\sigma}_{\alpha\mathbf{i}} \quad (1)$$

$$+\sum_{\alpha'\sigma'}V_{\alpha\alpha'}\hat{n}^\sigma_{\alpha\mathbf{i}}\hat{n}^{\sigma'}_{\alpha'\mathbf{i}}\Bigg],$$

$$\hat{H}_{pd}=\sum_{\langle ir\rangle}\sum_{\alpha\lambda\sigma\sigma'}(t_{\lambda\alpha}\hat{p}^+_{\alpha\mathbf{i}\sigma}\hat{d}_{\lambda\mathbf{r}\sigma}+\text{H.c.}+V_{\alpha\lambda}\hat{n}^\sigma_{\alpha\mathbf{i}}\hat{n}^{\sigma'}_{\lambda\mathbf{r}}),$$

$$\hat{H}_{pp}=\sum_{\langle i,j\rangle}\sum_{\alpha\beta\sigma}(t_{D\beta}\hat{p}^+_{\alpha\mathbf{i}\sigma}\hat{p}_{\beta\mathbf{j}\sigma}+\text{H.c.}),$$

where $\hat{n}^\sigma_{\lambda r}=\hat{d}^+_{\lambda r\sigma}\hat{d}_{\lambda r\sigma}$ and $\hat{n}^\sigma_{\alpha i}=\hat{p}^+_{\alpha i\sigma}\hat{p}_{\alpha i\sigma}$; indices **r** and **i**(**j**) run through the positions d_x, d_{3y}, p_{1x}, p_{2x}, p_z in sublattice *A* and d_y, d_{3x}, p_{1y}, p_{2y}, p_z in sublattice *B* of localized atomic orbitals; by the same token, $\varepsilon_\lambda=\varepsilon_{d_x}$ ($\lambda=d_x, d_{3x}, d_y, d_{3y}$) and $\varepsilon_\alpha=\varepsilon_p$ ($\alpha=p_x, p_y, p_z$) are the energies of the corresponding Mn3*d* and O2*p* atomic orbitals; the hopping matrix elements are t_{pd} for the orbitals $\lambda=d_x, d_y$; $\alpha=p_x, p_y, p_z$ and $2t_{pd}/\sqrt{3}$ for the orbitals $\lambda=d_{3x}, d_{3y}$; $\alpha=p_x, p_y$;

$$U_\lambda=\begin{cases}U_d, & \lambda=\lambda',\\ V_{dd}, & \lambda\neq\lambda',\end{cases}\quad(\lambda=d_x,d_y,d_{3x},d_{3y}),$$

$$U_\alpha=\begin{cases}U_p, & \alpha=\alpha',\\ V_{pp}, & \alpha\neq\alpha'\end{cases}\quad(\alpha=p_x,p_y,p_z)$$

are the intraatomic Coulomb interactions; and $V_{\alpha\lambda}=V_{pd}$ are the energies of Coulomb repulsion between manganese and oxygen. For simplicity, we assume in what follows that all matrix elements of the Coulomb and exchange interactions are independent of the form of *d* and *p* orbitals, that is, $U_d=V_{dd}$ and $U_p=V_{pp}$. In order to transform the above Hamiltonian to the basis in a cell centered on the manganese ion, we use a Fourier transform procedure defined as

$$\hat{d}_{\lambda\mathbf{k}\sigma}=\frac{1}{\sqrt{N}}\sum_{\mathbf{f}}\hat{d}_{\lambda\mathbf{f}\sigma}e^{-i\mathbf{k}\cdot\mathbf{f}},$$
$$\hat{p}_{\alpha\mathbf{k}\sigma}=\frac{1}{\sqrt{N}}\sum_{\mathbf{m}}\hat{p}_{\alpha\mathbf{m}\sigma}e^{-i\mathbf{k}\cdot\mathbf{m}} \quad (2)$$

and pass to a symmetric basis set of oxygen orbitals by constructing the new Wannier type functions using a linear transform of p_x, p_y, p_z atomic orbitals:

$$\begin{pmatrix}\hat{b}_\mathbf{k}\\ \hat{a}_\mathbf{k}\\ \hat{p}_\mathbf{k}\end{pmatrix}=\hat{A}\begin{pmatrix}\hat{p}_{x_1\mathbf{k}}\\ \hat{p}_{x_2\mathbf{k}}\\ \hat{p}_{z\mathbf{k}}\end{pmatrix}$$

$$=\begin{pmatrix}e^{ik^+}/\mu^b_k & e^{-ik^+}/\mu^b_k & 2c_z/\mu^b_k\\ 2c_z/\mu^a_k & 2c_z/\mu^a_k & -2\cos(k^+)/\mu^a_k\\ \dfrac{\operatorname{sgn}(k^+)\theta_{x_1k}}{\mu^p_k} & -\dfrac{\operatorname{sgn}(k^+)\theta_{x_2k}}{\mu^p_k} & -\dfrac{\operatorname{sgn}(k^+)4ic_zs_{k^+}}{\mu^{a^2}_k\mu^p_k}\end{pmatrix} \quad (3)$$

$$\times\begin{pmatrix}\hat{p}_{x_1\mathbf{k}}\\ \hat{p}_{x_2\mathbf{k}}\\ \hat{p}_{z\mathbf{k}}\end{pmatrix}.$$

Here, μ^a_k, μ^b_k, and μ^p_k are the normalization coefficients determined from the condition $\langle\hat{c}^+_\mathbf{k}|\hat{c}'_\mathbf{p}\rangle=\delta_{\mathbf{k}\cdot\mathbf{p}}\delta_{cc'}$, where $\hat{c}_\mathbf{k}=\hat{b}_\mathbf{k}, \hat{a}_\mathbf{k}, \hat{p}_\mathbf{k}$. This yields

$$\mu^a_\mathbf{k}=\sqrt{2c_z^2+c_+^2},\quad \mu^b_\mathbf{k}=\sqrt{\frac{1}{2}+c_z^2},$$
$$\mu^p_\mathbf{k}=\frac{1}{\mu^{a^2}_\mathbf{k}}\sqrt{2|\theta_\mathbf{k}|^2+c_z^2s_+^2}, \quad (4)$$

where

$$\theta_{x_1\mathbf{k}}=\frac{1}{\mu^{a^2}_k}\Bigg((c_z^2+c_+^2)\exp\left(\frac{ik^+}{4}\right)$$
$$+(c_z^2)\exp\left(-\frac{ik^+}{4}\right)\Bigg),$$
$$\theta_{x_2\mathbf{k}}=\theta^*_{x_1\mathbf{k}},\quad k^\pm=k_x\pm k_y.$$

In order to simplify writing, we use the following notation: $c_z=\cos(k_z/2)$, $c_\pm=\cos(k^\pm/4)$, and $s_\pm=\sin(k^\pm/2)$.

Formula (3) determines the oxygen states in sublattice *A*. In order to perform an analogous procedure for sublattice *B*, it is necessary to substitute $x\longleftrightarrow y$ in the notation of initial atomic orbitals and substitute $k^+\longleftrightarrow k^-$ in the transformation matrix $\hat{A}$. We use the coordinate system $\mathbf{k}=\mathbf{k}_x+\mathbf{k}_y+\mathbf{k}_z$, where $\mathbf{k}_x=(k'_x+k'_y)/2$, $\mathbf{k}_y=(k'_x-k'_y)/2$, $\mathbf{k}=\mathbf{k}'_z$ (prime refers to the initial coordinate system of the undistorted cubic structure). The

distance between nearest neighbor manganese ions is assumed to be the same in three directions: $a_x = a_y = a_z = 1$.

As will be seen below, the new oxygen $b(a)$ orbitals mix well in a separate cell with d_x (d_{3y}) states. For this reason, we employ the notation usually introduced for the irreducible representations in which the d_x (d_{3y}) orbitals are transformed. Writing the Hamiltonian in the new representation and separating the intracell and intercell interactions in the respective terms, we obtain:

$$\hat{H} = \hat{H}_0 + \hat{H}_{cc},$$

where

$$\hat{H}_0 = \sum_{G=A,B}\sum_{\mathbf{f}\sigma}(\hat{h}_G^{(a)} + \hat{h}_G^{(b)} + \hat{h}_G^{(ab)}),$$

$$\hat{h}_A^{(b)} = (\varepsilon_b\hat{n}_b^\sigma + \sigma_p\hat{n}_p^\sigma + \varepsilon_{d_x}\hat{n}_{d_x}^\sigma) + \frac{1}{2}U_d\hat{n}_{d_x}^\sigma\hat{n}_{d_x}^{-\sigma}$$

$$+\frac{1}{2}U_p\sum_{\alpha=b,p}\hat{n}_\alpha^\sigma\hat{n}_\alpha^{-\sigma}$$

$$+V_{pd}\sum_{\alpha=b,p}\sum_{\sigma'}\hat{n}_{d_x}^\sigma\hat{n}_\alpha^{\sigma'} + 2t_{pd}\mu_{000}^b(\hat{d}_{x\sigma}^+\hat{b}_\sigma + \text{H.c.})$$

$$-2t_{pp}\gamma_{000}^{bp}(\hat{b}_\sigma^+\hat{p}_\sigma + \text{H.c.}),$$

$$\hat{h}_A^{(a)} = (\varepsilon_a\hat{n}_a^\sigma + \varepsilon_{d_{3y}}\hat{n}_{d_{3y}}^\sigma) \qquad (5)$$

$$+\frac{1}{2}U_d\hat{n}_{d_{3y}}^\sigma\hat{n}_{d_{3y}}^{-\sigma} + \frac{1}{2}U_a\hat{n}_a^\sigma\hat{n}_a^{-\sigma}$$

$$+\sum_{\sigma'}V_{pd}\hat{n}_{d_{3y}}^\sigma\hat{n}_a^{\sigma'} - \frac{2t_{pd}\lambda_{000}}{\sqrt{3}}(\hat{d}_{3y\sigma}^+a_\sigma + \text{H.c.}),$$

$$\hat{h}_A^{(ab)} = U_d\sum_{\sigma'}\hat{n}_{d_x}^\sigma\hat{n}_{d_{3y}}^{\sigma'} + U_{ab}\hat{n}_a^\sigma\hat{n}_b^{\sigma'} + V_{pd}\hat{n}_{d_x}^\sigma\hat{n}_a^{\sigma'}$$

$$+V_{pd}\hat{n}_b^\sigma\hat{n}_{d_{3y}}^{\sigma'} + \frac{2t_{pd}\xi_{000}}{\sqrt{3}}(\hat{d}_{3y\sigma}^+b_\sigma + \text{H.c.})$$

$$-\frac{2t_{pd}\beta_{000}}{\sqrt{3}}(\hat{d}_{3y\sigma}^+p_\sigma + \text{H.c.}).$$

Here, $\varepsilon_b = \varepsilon_p^0 - 2t_{pp}\gamma_{000}^{bb}$, $\varepsilon_a = \varepsilon_p^0 + 2t_{pp}\gamma_{000}^{aa}$, and $\varepsilon_p = \varepsilon_p^0 - 2t_{pp}\gamma_{000}^{pp}$; for brevity, the site index $\mathbf{f}$ is omitted. Taking into account the relation $|\mu_{000}^b = 0.983| > |\xi_{000} = -0.0713|$, which corresponds to a weak *ab* hybridization in each cell, we can subdivide intercell terms in the same manner as

$$\hat{H}_{cc} = \sum_{GP}\sum_{\langle\mathbf{ij}\rangle\sigma}[(\hat{h}_{GP}^a + \hat{h}_{GP}^b + \hat{h}_{GP}^{ab})\delta_{GP} + \hat{h}_{GP}(1-\delta_{GP})], \qquad (6)$$

$$\hat{h}_{AA}^{(b)} = 2t_{pd}\mu_{\mathbf{ij}}^b(\hat{d}_{x\mathbf{i}\sigma}^+\hat{b}_{\mathbf{j}\sigma} + \text{H.c.}) - 2t_{pp}\gamma_{\mathbf{ij}}^{bb}\hat{b}_{\mathbf{i}\sigma}^+\hat{b}_{\mathbf{j}\sigma}$$

$$+2t_{pp}\gamma_{\mathbf{ij}}^{pp}\hat{p}_{\mathbf{i}\sigma}^+\hat{p}_{\mathbf{j}\sigma} - 2t_{pp}\gamma_{\mathbf{ij}}^{bp}(\hat{b}_{\mathbf{i}\sigma}^+\hat{p}_{\mathbf{j}\sigma} + \text{H.c.}),$$

$$\hat{h}_{AA}^{(a)} = 2\frac{t_{pd}\lambda_{\mathbf{ij}}}{\sqrt{3}}(\hat{d}_{3y\mathbf{i}\sigma}^+\hat{a}_{\mathbf{j}\sigma} + \text{H.c.}) + 2t_{pp}\gamma_{\mathbf{ij}}^{aa}\hat{a}_{\mathbf{i}\sigma}^+\hat{a}_{\mathbf{j}\sigma},$$

$$\hat{h}_{AA}^{(ab)} = 2\frac{t_{pd}\xi_{ij}}{\sqrt{3}}(\hat{d}_{3y\mathbf{i}\sigma}^+\hat{b}_{\mathbf{j}\sigma} + \text{H.c.})$$

$$+2\frac{t_{pd}\beta_{ij}}{\sqrt{3}}(\hat{d}_{3y\mathbf{i}\sigma}^+\hat{b}_{\mathbf{j}\sigma} + \text{H.c.}) - 2t_{pp}\gamma_{\mathbf{ij}}^{ab}(\hat{a}_{\mathbf{i}\sigma}^+\hat{b}_{\mathbf{j}\sigma} + \text{H.c.})$$

for the hops within one sublattice, and

$$h_{GP} = -2\left(\frac{t_{pd}}{\sqrt{3}}\right)\hat{d}_{3y\mathbf{i}\sigma}^{+(G)}\sum_{c=a,b,p}(\alpha_{\mathbf{ij}}^{c(P)}\hat{c}_{\mathbf{j}\omega}^{(P)} + \text{H.c.})$$

for the intersublattice hopping. The coefficients μ^b, λ, ξ, and β for intrasublattice *pd* interactions; $\alpha^{a(G)}$, $\alpha^{b(G)}$, and $\alpha^{p(G)}$ for the intersublattice *pd* interactions; and γ^{aa}, γ^{bb}, γ^{pp}, γ^{ab}, γ^{bp}, and γ^{ap} for the intrasublattice *pp* interactions as functions of the distance between cells are presented in the table, where $[m, n, l]$ denotes the coordinates of the **j**th cells relative to the **i**th cell. For example, 1 = [1/2, 1/2, 0] denotes a cell occurring in the first coordination sphere of the **i**th cell, but belonging to another sublattice; 2 = [1, 0, 0] denotes a cell occurring in the second coordination sphere of the **i**th cell and belonging to the same sublattice.

In the Hamiltonian written as above, the term $\hat{H}_0$ contains all *pd* and *pp* hybridization (hopping), Coulomb interactions, and exchange interactions inside the cell. As can be seen from the table, the coefficients rapidly decay with the distance. For this reason, we leave only the *pd* and *pp* hybridization interactions in $\hat{H}_{cc}$ and omit the Coulomb and exchange interactions between cells. The omitted terms are small as compared to the intracell interactions [16]; they renormalize these interactions and lead to more complicated hops involving three and four cells [11].

3. CONSTRUCTING A CONFIGURATION SPACE OF THE ELECTRON SUBSYSTEM ON THE BASIS OF HIGH-SPIN STATES (S = 5/2, 2, 3/2)

Hamiltonian $\hat{H}_0$ can be diagonalized in the space of many-particle functions corresponding to all possible

Coefficients of inter- and intrasublattice interactions

	0 = [0, 0, 0]	2 = [1, 0, 0]	1 = [1/2, 1/2, 0]	1 = [1/2, –1/2, 0]	1 = [0, 0, 1]
			For *pd* interactions in sublattices *A* and *B*		
μ_{mnl}	0.9833	0.0466			0.1282
λ_{mnl}	0.7482	0.0704			0.1641
ξ_{mnl}	–0.0713	0.0034			–0.2708
β_{mnl}	0.0000	0.0000			0.0000
			For *pp* interactions in sublattices *A* and *B*		
γ^{bb}_{mnl}	0.4226	0.0200			0.1547
γ^{aa}_{mnl}	0.3287	0.0398			0.1125
γ^{pp}_{mnl}	0.0235	–0.0049			0.0106
γ^{ab}_{mnl}	0.0907	0.0096			0.1157
γ^{ap}_{mnl}	0.3037	0.0251			–0.1502
γ^{ap}_{mnl}	0.0000	0.0000			0.0000
			For *pd* interactions between sublattices *A* and *B*		
$\alpha^{b(G)}_{mnl}$			–0.1426, $G = A$ 0, $G = B$	–0.1426, $G = B$ 0, $G = A$	
$\alpha^{a(G)}_{mnl}$			0.0286, $G = A$ 0, $G = B$	0.0286, $G = B$ 0, $G = A$	
$\alpha^{p(G)}_{mnl}$			0.0325, $G = A$ 0, $G = B$	0.0325, $G = B$ 0, $G = A$	

distributions of electrons over one-particle states. The operators of *d* electron production can be written in terms of Hubbard operators in the space of many-particle *d* states $|e_g^2, M_{5/2}\rangle$, $|h_{d_x}, M_2\rangle$, $|h_{d_{3y}}, M_2\rangle$, $|t_{2g}^3, M_{3/2}\rangle$ (see Eqs. (8), (9), and (11):

$$\hat{d}^+_{\mathbf{f}\chi\sigma} = \sum_{M=-2}^{2} \begin{pmatrix} u_1(M) \\ v_1(M) \end{pmatrix} \hat{X}^{|h_{d,-\chi,M}\rangle\langle t^3_{2g}, M-\sigma|}_{\mathbf{f}} + \sum_{M=-5/2}^{5/2} \chi \begin{pmatrix} u_2(M) \\ v_2(M) \end{pmatrix} \hat{X}^{|e^2_g, M\rangle\langle h_{d,\chi}, M-\sigma|}_{\mathbf{f}}, \quad (7)$$

where

$$\chi = \begin{cases} +1, & \lambda = x, y, \\ -1, & \lambda = 3x, 3y \end{cases}$$

(the upper and lower lines refer to the states with spin $\sigma = \uparrow$ and $\sigma = \downarrow$, respectively), and

$$u_1^2(M) = \frac{2+M}{4}, \quad v_1^2(M) = \frac{2-M}{4},$$

$$u_2^2(M) = \frac{5/2+M}{5}, \quad v_2^2(M) = \frac{5/2-M}{5}.$$

These operators act only on electrons occurring in the e_g shell, but it does not act on t_{2g} electrons. As a result, the Hamiltonian of the whole system corresponds to the transfer of spin density from the e_g shell to ligands, while $S = 3/2$ on the t_{2g} shell. The resultant spin is constructed in accordance with the Hund rule. Using the above operators, it is possible to construct many-particle functions corresponding to the following parts of the configuration space:

(i) a high-spin sector d^5p^6 ($S = 5/2$) with a half-filled $t_{2g}^3 e_g^2$ Mn3*d* shell (quasi-particle "vacuum" sector);

(ii) an one-hole sector, where the ground state is formed by split states of the ${}^5e_g$ spin multiplet repre-

senting a combination of d^4p^6 and d^5p^5 ($S = 2$) configurations;

(iii) a two-hole sector, where the ground state is a linear combination of the d^3p^6, d^4p^5, and d^5p^4 ($S = 3/2$) configurations.

In the one-hole sector, we deal with two spin multiplets, ^5a and ^5b, possessing different orbital symmetry and a small mutual hybridization because a and b states can mix in the presence of a $\sqrt{2} \times \sqrt{2}$ superlattice. The hole can occur on any of the Mn3d or O2p orbitals. Introducing a notation for the half-filled d shell as

$$|e_g^2, M_{S=5/2}\rangle$$
$$= u_2(M_{5/2})\Big[u_1\Big(M_{5/2}-\frac{1}{2}\Big)d^+_{x\uparrow}d^+_{3y\uparrow}|t_{2g}^3, M_{5/2}-1\rangle$$
$$+ v_1\Big(M_{5/2}-\frac{1}{2}\Big)d^+_{x\downarrow}d^+_{3y\uparrow}|t_{2g}^3, M_{5/2}\rangle\Big]$$
$$+ v_2(M_{5/2})\Big[u_1\Big(M_{5/2}+\frac{1}{2}\Big)d^+_{x\uparrow}d^+_{3y\downarrow}|t_{2g}^3, M_{5/2}\rangle$$
$$+ v_1\Big(M_{5/2}+\frac{1}{2}\Big)d^+_{x\downarrow}d^+_{3y\downarrow}|t_{2g}^3, M_{5/2}+1\rangle\Big]$$

and $|d_\chi, M_{S=2}\rangle$ (see (8)) for the state with a hole in one of the e_g states, and applying operator (7) with an additional normalization condition, it is possible to complete the set of many-particle functions as

$$|h_b, M_2\rangle$$
$$= \alpha_{5/2}[u_2(M_2+1/2)|e_g^2, M_2+1/2\rangle|a^2, p^2, b_\downarrow\rangle$$
$$- v_2(M_2-1/2)|e_g^2, M_2-1/2\rangle|a^2, p^2, b_\uparrow\rangle],$$
$$|h_{d_x}, M_2\rangle = \{u_1(M_2)d^+_{3y\uparrow}|t_{2g}^3, M_2-1/2\rangle$$
$$+ v_1(M_2)d^+_{3y\downarrow}|t_{2g}^3, M_2+1/2\rangle\}|p^6\rangle, \quad (8)$$
$$|h_p, M_2\rangle$$
$$= \alpha_{5/2}[u_2(M_2+1/2)|e_g^2, M_2+1/2\rangle|a^2, p_\downarrow, b^2\rangle$$
$$- v_2(M_2-1/2)|e_g^2, M_2-1/2\rangle|a^2, p_\uparrow, b^2\rangle]$$

for a single hole in the initial block b, and as

$$|h_a, M_2\rangle$$
$$= \alpha_{5/2}[u_2(M_2+1/2)|e_g^2, M_2+1/2\rangle|a_\downarrow, p^2, b^2\rangle$$
$$- v_2(M_2-1/2)|e_g^2, M_2-1/2\rangle|a_\uparrow, p^2, b^2\rangle], \quad (9)$$
$$|h_{d_{3Y}}, M_2\rangle = \{u_1(M_2)d^+_{x\uparrow}|t_{2g}^3, M_2-1/2\rangle$$
$$+ v_2(M_2)d^+_{x\downarrow}|t_{2g}^3, M_2+1/2\rangle\}|p^6\rangle,$$

for a hole in the initial block a. In these expressions,

$$\alpha_{5/2} = \sqrt{\frac{2S_{5/2}}{2S_{5/2}+1}}$$

is the normalization of the wave functions in the cell with a hole on oxygen orbitals; $u_i(M_2)$ and $v_i(M_2)$ are the vector slip coefficients, which appear upon expansion of the wave function in the one-hole sector in terms of the wave functions of the configuration with $S = 3/2$ and the function of an additional oxygen with $\sigma = 1/2$ in one of the possible states.

Thus, in the one-hole sector with the basis $|h_a, M_2\rangle$, $|d_{3y}, M_2\rangle$, and $|h_{d_x}, M_2\rangle$, $|h_b, M_2\rangle$, $|h_p, M_2\rangle$, we determined the eigenstates $|1h_{iM_2}\rangle = \sum_c \beta_i(c)|h_c, M_2\rangle$ ($c = a, d_{3x}, b, p, d_x$) with the energies ε_{iM_2} ($i = 1, \ldots, 5$) by means of the exact diagonalization of the matrix

$$\begin{pmatrix} E_{d_x} & \alpha_{5/2}\tau_b & 0 & 0 & 0 \\ \alpha_{5/2}\tau_b & E_b & \alpha_{5/2}\tau_{db} & \tau_{ab} & \tau_{bp} \\ 0 & \alpha_{5/2}\tau_{db} & E_{d_{3x}} & \alpha_{5/2}\tau_a & 0 \\ 0 & \tau_{ab} & \alpha_{5/2}\tau_a & E_a & 0 \\ 0 & \tau_{bp} & 0 & 0 & E_p \end{pmatrix}\sigma_{M_2, M_2'}, \quad (10)$$

where

$$\tau_b = 2t_{pd}\mu_{00}, \quad \tau_a = -\frac{2}{\sqrt{3}}t_{pd}\lambda_{000}, \quad \tau_{ab} = -2t_{pp}\gamma^{bp}_{000},$$
$$\tau_{bp} = -2t_{pp}\gamma^{bp}_{000}, \quad \tau_{ap} = -2t_{pp}\gamma^{ap}_{000} \approx 0,$$
$$\tau_{dp} = \frac{2}{\sqrt{3}}t_{pd}\beta_{000} \approx 0, \quad \tau_{dp} = -\frac{2}{\sqrt{3}}t_{pd}\xi_{000},$$
$$E_{d_x} = \varepsilon_{d_{3x}} + 2(\varepsilon_a + \varepsilon_p + \varepsilon_b) + 3U_p + 6V_{pd} + 12V_{pp},$$
$$E_b = \varepsilon_{d_z} + \varepsilon_{d_x} + 2(\varepsilon_a + \varepsilon_p) + \varepsilon_b$$
$$+ U_d - J_H + 2U_p + 10V_{pd} + 8V_{pp},$$
$$E_p = \varepsilon_{d_z} + \varepsilon_{d_x} + 2(\varepsilon_a + \varepsilon_b) + \varepsilon_p$$
$$+ U_d - J_H + 2U_p + 10V_{pd} + 8V_{pp},$$
$$E_{d_{3y}} = \varepsilon_{d_z} + 2(\varepsilon_a + \varepsilon_p + \varepsilon_b) + 3U_p + 6V_{pd} + 12V_{pp},$$
$$E_a = \varepsilon_{d_z} + \varepsilon_{d_x} + 2(\varepsilon_p + \varepsilon_b) + \varepsilon_a$$
$$+ U_d - J_H + 2U_p + 10V_{pd} + 8V_{pp}.$$

In accordance with five possible spin projections ($M_2 = -2, \ldots, +2$), each position splits into five possible variants.

The initial basis for the two-hole sector ($S = 3/2$) is as follows:

$$
\begin{aligned}
|h_{d_x}, h_a, M_{3/2}\rangle &= \alpha_2\{u_1(M_{3/2}+1/2)\\
&\times|d_{3y}, M_{3/2}+1/2\rangle|a_\downarrow p^2 b^2\rangle\\
&+ v_1(M_{3/2}-1/2)|d_{3y}, M_{3/2}-1/2\rangle|a_\uparrow p^2 b^2\rangle\},\\
|h_{d_x}, h_p, M_{3/2}\rangle &= \alpha_2\{u_1(M_{3/2}+1/2)\\
&\times|d_{3y}, M_{3/2}+1/2\rangle|a^2 p_\downarrow b^2\rangle\\
&+ v_1(M_{3/2}-1/2)|d_{3y}, M_{3/2}-1/2\rangle|a^2 p_\uparrow b^2\rangle\},\\
|h_{3y}, h_b, M_{3/2}\rangle &= \alpha_2\{u_1(M_{3/2}+1/2)\\
&\times|d_x, M_{3/2}+1/2\rangle|a^2 p^2 b_\downarrow\rangle\\
&+ v_1(M_{3/2}-1/2)|d_x, M_{3/2}-1/2\rangle|a^2 p^2 b_\uparrow\rangle\},\\
|h_{d_x}, h_{d_{3y},M_{3/2}}\rangle &= |t_{2g}^3, M_{3/2}\rangle|p^6\rangle,\\
|h_a, h_b, M_{3/2}\rangle&\\
= \alpha_2\alpha_{5/2}\{&u_1(M_{3/2}+1)u_1(M_{3/2}+1/2)\\
&\times|e_g^2, M_{3/2}+1\rangle|a_\downarrow, p^2, b_\downarrow\rangle\\
&- u_2(M_{3/2})v_1(M_{3/2}-1/2)|e_g^2, M_{3/2}\rangle|a_\downarrow, p^2, b_\uparrow\rangle\\
&- v_2(M_{3/2})u_1(M_{3/2}+1/2)|e_g^2, M_{3/2}\rangle|a_\uparrow, p^2, b_\downarrow\rangle\\
&+ v_2(M_{3/2}-1)v_1(M_{3/2}-1/2)|e_g^2, M_{3/2}-1\rangle\\
&\times|a_\uparrow, p^2, b_\downarrow\rangle\},\\
|h_p, h_b, M_{3/2}\rangle&\\
= \alpha_2\alpha_{5/2}\{&u_2(M_{3/2}+1)u_1(M_{3/2}+1/2)\\
&\times|e_g^2, M_{3/2}+1\rangle|a^2, p_\downarrow, b_\downarrow\rangle\\
&- u_2(M_{3/2})v_1(M_{3/2}-1/2)|e_g^2, M_{3/2}\rangle|a^2, p_\downarrow, b_\uparrow\rangle\\
&- v_2(M_{3/2})u_1(M_{3/2}+1/2)|e_g^2, M_{3/2}\rangle|a^2, p_\uparrow, b_\downarrow\rangle\\
&+ v_2(M_{3/2}-1)v_1(M_{3/2}-1/2)|e_g^2, M_{3/2}-1\rangle\\
&\times|a^2, p_\uparrow, b_\uparrow\rangle\},
\end{aligned}
\tag{11}
$$

where

$$\alpha_2 = \sqrt{\frac{2S_2}{2S_2+1}},$$

and the left-hand part also makes use of the "hole" notations. In this sector, the eigenstates can be found in the following form: $|2h_{iM_{3/2}}\rangle = \sum_{cc'} B_i(c, c')\,|h_C, H_{C'}, M_{3/2}\rangle$, where the energies $\varepsilon_{iM_{3/2}}$ and the corresponding coefficients B_{iq} ($q = 1, \ldots, 6$) are determined by diagonalization of the matrix

$$
\begin{pmatrix}
E_{ad_x} & -\alpha_{5/2}\tau_b & \alpha_2\tau_a & 0 & 0 & 0 & 0 & 0 & 0 & \tau_{ab}\\
-\alpha_{5/2}\tau_b & E_{ab} & 0 & \alpha_{5/2}\tau_a & 0 & 0 & -\alpha_{5/2}\tau_{bd} & \tau_{bp} & 0 & 0\\
\alpha_2\tau_a & 0 & E_{dd} & -\alpha_2\tau_b & 0 & 0 & 0 & 0 & 0 & \alpha_2\tau_{bd}\\
0 & \alpha_{5/2}\tau_a & -\alpha_2\tau_b & E_{bd_{3x}} & 0 & 0 & \tau_{ab} & 0 & \tau_{bp} & 0\\
0 & 0 & 0 & 0 & E_{pd_x} & -\alpha_{5/2}\tau_b & 0 & 0 & 0 & \tau_{bp}\\
0 & 0 & 0 & 0 & -\alpha_{5/2}\tau_b & E_{pb} & 0 & -\tau_{ab} & -\alpha_{5/2}\tau_{bd} & 0\\
0 & -\alpha_{5/2}\tau_{bd} & 0 & \tau_{ab} & 0 & 0 & E_{ad_{3x}} & 0 & 0 & 0\\
0 & \tau_{bp} & 0 & 0 & 0 & -\tau_{ab} & 0 & E_{ap} & \alpha_{5/2}\tau_a & 0\\
0 & 0 & 0 & \tau_{bp} & 0 & -\alpha_{5/2}\tau_{bd} & 0 & \alpha_{5/2}\tau_a & E_{pd_{3x}} & 0\\
\tau_{ab} & 0 & \alpha_2\tau_{bd} & 0 & \tau_{bp} & 0 & 0 & 0 & 0 & R_{bd_x}
\end{pmatrix}
\times\delta_{M_{3/2}M'_{3/2}}
\tag{12}
$$

with a total dimension of 40×40 for the direct matrix product. Using the results of exact diagonalization, the configuration space of the system is reduced to that depicted in Fig. 2 with two orbitally nondegenerate (a and b) terms in the one-hole sector. The other terms possess much higher energies and are insignificant

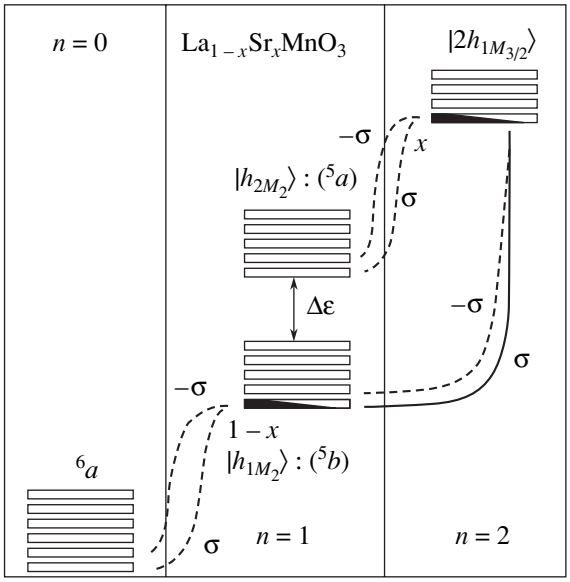

Fig. 2. Schematic diagram of the configuration space of charge carriers in $La_{1-x}Sr_xMnO_3$, showing transitions corresponding to the valence band (solid curve) and the bands of in-gap states (dashed curves) and indicating the spins of quasiparticles involved in these transitions; $n = 0$, 1, and 2 correspond to the vacuum and the one- and two-particle sectors; $|h_{1M_2}\rangle$ and $|h_{2M_2}\rangle$ are the mixing ^5b and ^5a states; $|2h_{1M_{3/2}}\rangle$ is the ground state in the two-hole sector. See the text for the notation of states.

from the standpoint of low-energy excitations. Depending on the parameters of Hamiltonian H, the splitting of weakly mixing orbital ^5a and ^5b singlets is on the order of $\Delta\varepsilon \approx 0.2$–$0.5$ eV. The existence of two states, $|1h_{1M_2}\rangle$ and $|1h_{2M_2}\rangle$, with close energies implies the need for their simultaneous inclusion into the basis set for our calculation. Therefore, the Hamiltonian cannot be further reduced to an affective one-band model. In contrast to the case of cuprates [11], the presence of a large spin $S = 3/2$ on the t_{2g} shell in the two-hole sector corresponds to a situation with a single high-spin term separated from the excited terms by a energy interval of ~1 eV. This state is analogous to the Zhang–Rice state in cuprates. Thus, we obtained a new reduced basis set of high-spin functions in the cell, which determines the low-energy excitations of the electron system in $LaMnO_3$.

4. DERIVING DISPERSION RELATIONS

The hopping part $\hat{H}_{cc}$ of the total Hamiltonian is conveniently treated using a representation of Hubbard operators analogous to (7), which is determined in the space of many-electron functions (8), (9), and (11). Any one-electron operator can be written using Hubbard operators $\hat{X}_f^{pq} = |p\rangle\langle q|$ as

$$\hat{c}_{\lambda\mathbf{f}\sigma} = \sum_m \gamma_{\lambda\sigma}(m)\hat{X}_{\mathbf{f}}^m,$$

where

$$\hat{c}_{\lambda\mathbf{f}\sigma} = \hat{d}_{x\mathbf{f}\sigma}, \hat{d}_{z\mathbf{f}\sigma}, \hat{a}_{\mathbf{f}\sigma}, \hat{b}_{\mathbf{f}\sigma}, \hat{p}_{z\mathbf{f}\sigma}$$

and m is the number index of the root vector $\boldsymbol{\alpha}_m(pq)$. The work with Hubbard operators is simplified using Zaitsev notation [22], whereby each pair of the initial and final states, $|q\rangle \longrightarrow |p\rangle$, corresponds to a root vector $\boldsymbol{\alpha}_m(pq)$ such that

$$\hat{X}_{\mathbf{f}}^{pq} \longrightarrow \hat{X}_{\mathbf{f}}^{\boldsymbol{\alpha}_m(pq)} \longrightarrow \hat{X}_{\mathbf{f}}^m,$$

where superscripts p and q enumerate the states in (8), (9), and (11). Then, the matrix elements of the hopping amplitude $\gamma_{\lambda\sigma}(m) = \langle p|\hat{c}_{\lambda\mathbf{f}\sigma}|q\rangle$ ($m = 1, 2, \ldots, 400$ in an orbitally ordered AFM phase) corresponding to these root vectors are directly calculated using the coefficients $B_i(c, c')$ and $\beta_i(c)$ and represent the partial amplitudes of transitions between individual many-electron states. In contrast to Hubbard operators, the operators of production (annihilation) act on the states in all sectors of the configuration space of the system.

Spin multiplets comprising the set of many-electron states (8), (9), and (11) can belong to various orbital and magnetic sublattices and, in agreement with the existence of two orbital sublattices A and B, we introduce vectors $\mathbf{R}_1$ for the intrasublattice neighbors and $\mathbf{R}_2$ for the intersublattice ones. In the AFM phase, each of the two orbital sublattices consists of two magnetic sublattices alternating along the z axis. The magnetic sublattice features FM ordering in the xy plane, which corresponds to the A-type AFM ordering observed in $LaMnO_3$. Since the introduction of various sublattices presents only technical problems, we will restrict the consideration to deriving the dispersion equation for an orbitally ordered homogeneous magnetic state, that is, for a system with PM and FM phases. In this case, the Hamiltonian of intercell hopping can be written as

$$\hat{H}_{cc} = \sum_{G,P} \hat{H}_{cc}^{GP}$$

$$= \sum_{\mathbf{f}} \sum_{\lambda\lambda'\sigma} \left\{ \sum_{\mathbf{R}_1} \sum_G T_{\lambda\lambda'}^G(\mathbf{R}_1)(\hat{c}_{\mathbf{f}\lambda\sigma}^{+(G)} \hat{c}_{\mathbf{f}+\mathbf{R}_1\lambda'\sigma}^{(G)} + \text{H.c.}) \right.$$

$$+\sum_{\mathbf{R}_2}\sum_{G\neq P} T^{GP}_{\lambda\lambda'}(\mathbf{R}_2)(\hat{c}^{+(G)}_{\mathbf{f}\lambda\sigma}\hat{c}^{(P)}_{\mathbf{f}+\mathbf{R}_2\lambda'\sigma}+\text{H.c.})\Big\}$$

$$=\sum_{\lambda\lambda'\sigma}\sum_{kmn}\{\gamma^*_{\lambda\sigma}(m)\gamma_{\lambda'\sigma}(n)[T^{AA}_{\lambda\lambda'}(\mathbf{k})\hat{X}^{+m}_{\mathbf{k}}\hat{X}^{n}_{\mathbf{k}}$$

$$+T^{BB}_{\lambda\lambda'}(\mathbf{k})\hat{Y}^{+m}_{\mathbf{k}}\hat{Y}^{n}_{\mathbf{k}}+T^{AB}_{\lambda\lambda'}(\mathbf{k})\hat{X}^{+m}_{\mathbf{k}}\hat{Y}^{n}_{\mathbf{k}}$$

$$+T^{BA}_{\lambda\lambda'}(\mathbf{k})\hat{Y}^{+m}_{\mathbf{k}}\hat{X}^{n}_{\mathbf{k}}]+\text{H.c.}\},\qquad(13)$$

where

$$T^{GG}_{\lambda\lambda'}(\mathbf{k})=\frac{2}{N}\sum_{\mathbf{R}_1}T^{GG}_{\lambda\lambda'}(\mathbf{R}_1)e^{i\mathbf{k}\cdot\mathbf{R}_1},$$

$$T^{GP}_{\lambda\lambda'}(\mathbf{k})=\frac{2}{N}\sum_{\mathbf{R}_2}T^{GP}_{\lambda\lambda'}(\mathbf{R}_2)e^{i\mathbf{k}\cdot\mathbf{R}_2}\neq T^{PG}_{\lambda\lambda'}(\mathbf{k})$$

(because $T^{AB}_{\lambda\lambda'}(\mathbf{k})$ and $T^{BA}_{\lambda\lambda'}(\mathbf{k})$ determine the dispersion in different $\mathbf{k}$ directions, see table); $\hat{X}^m_k$ and $\hat{Y}^n_k$ are the Fourier images of Hubbard operators for the orbital sublattices A and B, respectively. Within one sublattice, the hopping matrix on the basis d_x (d_y), d_{3y} (d_{3x}) of a, p, b orbitals with $T^G_{\lambda\lambda'}(\mathbf{R}_1)$ elements is

$$T^G_{\lambda\lambda'}(\mathbf{R}_1)=\begin{pmatrix}0 & 0 & 2t_{pd}\mu & 0 & 0\\ 0 & 0 & -2t_{pd}\xi/\sqrt{3} & -2t_{pd}\lambda/\sqrt{3} & 2t_{pd}\beta/\sqrt{3}\\ 2t_{pd}\mu & -2t_{pd}\xi/\sqrt{3} & -2t_{pp}\gamma^{bb} & -2t_{pp}\gamma^{ab} & -2t_{pp}\gamma^{bp}\\ 0 & 2t_{pd}\lambda\sqrt{3} & -2t_{pp}\gamma^{ab} & 2t_{pp}v & -2t_{pp}\gamma^{ap}\\ 0 & 2t_{pd}\beta/\sqrt{3} & -2t_{pp}\gamma^{bp} & -2t_{pp}\gamma^{ap} & -2t_{pp}\gamma^{pp}\end{pmatrix}.\qquad(14)$$

Accordingly, the matrix of intersublattice transitions with $T^{PG}_{\lambda\lambda'}(\mathbf{R}_2)$ elements is

$$T^{GP}_{\lambda\lambda'}(\mathbf{R}_2)=\begin{pmatrix}0 & 0 & 0 & 0 & 0\\ 0 & 0 & -2t_{pd}\alpha^{b(G)}/\sqrt{3} & -2t_{pd}\alpha^{a(G)}/\sqrt{3} & -2t_{pd}\alpha^{p(G)}/\sqrt{3}\\ 0 & -2t_{pd}\alpha^{b(G)}/\sqrt{3} & 0 & 0 & 0\\ 0 & -2t_{pd}\alpha^{a(G)}/\sqrt{3} & 0 & 0 & 0\\ 0 & -2t_{pd}\alpha^{p(G)}/\sqrt{3} & 0 & 0 & 0\end{pmatrix}.\qquad(15)$$

The equations of motion for operators X^m_f and Y^n_g can be written as

$$i\dot{\hat{X}}^m_{\mathbf{f}}=[\hat{X}^m_{\mathbf{f}},\hat{H}]=\Omega_m\hat{X}^m_{\mathbf{f}}+[\hat{X}^m_{\mathbf{f}},\hat{H}_{cc}],\qquad(16)$$

where $\Omega^G_m=\Omega^G(\boldsymbol{\alpha}_m)=\varepsilon^G_q-\varepsilon^G_p$. The corresponding commutator can be calculated in Hubbard 1 approximation as

$$[\hat{X}^m_{\mathbf{f}},\hat{H}_{cc}]=\sum_{\lambda\lambda'\sigma'}\sum_{nl}\sum_{i\mathbf{R}}T_{\lambda\lambda'}(\mathbf{R})$$

$$\times\{\gamma^*_{\lambda\sigma'}(n)\gamma_{\lambda'\sigma'}(l)[\hat{X}^m_{\mathbf{f}},\hat{X}^{+n}_{\mathbf{i}}\hat{X}^l_{\mathbf{i}+\mathbf{R}}]$$

$$+\gamma^*_{\lambda'\sigma'}(l)\gamma_{\lambda\sigma'}(n)[\hat{X}^m_{\mathbf{f}},\hat{X}^{+l}_{\mathbf{i}+\mathbf{R}}\hat{X}^n_{\mathbf{i}}]\}\qquad(17)$$

$$\approx\sum_{\lambda\lambda'n}\gamma^*_{\lambda\sigma}(m)\gamma_{\lambda'\sigma}(n)F_{\mathbf{f}}(m)$$

$$\times\sum_{\mathbf{R}}T_{\lambda\lambda'}(\mathbf{R})(\hat{X}^n_{\mathbf{f}+\mathbf{R}}+\hat{X}^n_{\mathbf{f}-\mathbf{R}}),$$

where $F_{\mathbf{f}}(m)=F_{\mathbf{f}}(\boldsymbol{\alpha}_m)=\langle\hat{X}^{pp}_{\mathbf{f}}\rangle+\langle\hat{X}^{qq}_{\mathbf{f}}\rangle$ is the filing factor. Taking into account the presence of two sublattices, we obtain the following system of equations:

$$i\dot{\hat{X}}^m_{\mathbf{f}}=\Omega^A_m\hat{X}^m_{\mathbf{f}}+\sum_{\lambda\lambda'n}\gamma^*_{\lambda\sigma}(m)\gamma_{\lambda'\sigma}(n)F_A(m)$$

$$\times\left(\sum_{\mathbf{R}_2}\hat{Y}^n_{\mathbf{f}+\mathbf{R}_2}[T^{AB}_{\lambda\dot{\lambda}}+T^{BA}_{\lambda\dot{\lambda}}]+2\sum_{\mathbf{R}_1}\hat{X}^n_{\mathbf{f}+\mathbf{R}_1}T^{AA}_{\lambda\lambda'}\right),$$

$$i\dot{\hat{Y}}^m_{\mathbf{g}}=\Omega^B_m\hat{Y}^m_{\mathbf{g}}+\sum_{\lambda\lambda'n}\gamma^*_{\lambda\sigma}(m)\gamma_{\lambda'\sigma}(n)F_B(m)\qquad(18)$$

$$\times\left(\sum_{\mathbf{R}_2}\hat{Y}^n_{\mathbf{g}+\mathbf{R}_2}[T^{AB}_{\lambda\dot{\lambda}}+T^{BA}_{\lambda\dot{\lambda}}]+2\sum_{\mathbf{R}_1}\hat{Y}^n_{\mathbf{g}+\mathbf{R}_1}T^{BB}_{\lambda\lambda'}\right).$$

This approximation is valid only provided that $\sum_{\lambda\lambda'}\gamma^*_{\lambda\sigma}(m)T^{PG}_{\lambda\lambda'}(\mathbf{k})\gamma_{\lambda'\sigma}(n) \ll \Omega^G_m$. In addition to the relation $\eta_{000} > \eta_{mnl}$ (where $\eta = \mu, \lambda, \xi, \beta$, and γ, see table), this condition introduces another small parameters of the obtained solution. Introducing a new notation for the effective interaction as

$$T^{PG}_{\text{eff},\,mn}(\mathbf{k},\sigma) = \begin{cases} \sum_{\lambda\lambda'}\gamma^*_{\lambda\sigma}(m)T^{GG}_{\lambda\lambda'}(\mathbf{k})\gamma_{\lambda'\sigma}(n), & G = P, \\ \frac{1}{2}\sum_{\lambda\lambda'}\gamma^*_{\lambda\sigma}(m)[T^{AB}_{\lambda\lambda'}(\mathbf{k}) + T^{BA}_{\lambda\lambda'}(\mathbf{k})]\gamma_{\lambda'\sigma}(n), & G \neq P, \end{cases}$$

we can use a more convenient matrix form of the equations of motion for the Green function

$$\hat{D}_{\mathbf{ij}} = \begin{pmatrix} \hat{D}_{\mathbf{ij}}(AA) & \hat{D}_{\mathbf{ij}}(AB) \\ \hat{D}_{\mathbf{ij}}(BA) & \hat{D}_{\mathbf{ij}}(BB) \end{pmatrix},$$

where

$$D^{mn}_{\mathbf{ij}}(AB) = \langle\langle \hat{X}^m_{\mathbf{i}} | \hat{Y}^n_{\mathbf{j}} \rangle\rangle.$$

Indeed, consider the system of equations

$$D^{mn}_{\mathbf{ij}}(AA) = D^0_m(A)\delta_{\mathbf{ij}}\delta_{mn} + 2D^0_m(A)\sum_{\lambda\lambda' l}\gamma^*_{\lambda\sigma}(m)\gamma_{\lambda'\sigma}(l)\left(\sum_{\mathbf{R}_2} T^{AB}_{\lambda\lambda'}D^{ln}_{\mathbf{i}+\mathbf{R}_2\mathbf{j}}(BA) + \sum_{\mathbf{R}_1} T^{AA}_{\lambda\lambda'}D^{ln}_{\mathbf{i}+\mathbf{R}_1\mathbf{j}}(AA)\right), \quad (19)$$

$$D^{mn}_{\mathbf{ij}}(BA) = D^0_m(B)\sum_{\lambda\lambda' l}\gamma^*_{\lambda\sigma}(m)\gamma_{\lambda'\sigma}(l) \times \left(\sum_{\mathbf{R}_2} T^{BA}_{\lambda\lambda'}D^{ln}_{\mathbf{i}+\mathbf{R}_1\mathbf{j}}(AA) + \sum_{\mathbf{R}_1} T^{BB}_{\lambda\lambda'}D^{ln}_{\mathbf{i}+\mathbf{R}_1\mathbf{j}}(BA)\right),$$

where

$$D^0_m(G) = \frac{F_G(m)}{E - \Omega^G_m + i\varepsilon}$$

is the Green function in the zero-order approximation. Applying the Flourier transform

$$D^{mn}_{ij} = \frac{2}{N}\sum_k D^{mn}_k e^{ik(\mathbf{R}_i - \mathbf{R}_j)},$$

and using the above notation for $T^{PG}_{\text{eff},\,mn}(\mathbf{k},\sigma)$, Eqs. (19) can be rewritten as

$$\begin{aligned} &\sum_l \{D^{ln}_{\mathbf{k}}(AA)[\delta_{ml} - 2D^0_m(A)T^{AA}_{\text{eff},\,ml}(\mathbf{k},\sigma)] \\ &- 2D^{ln}_{\mathbf{k}}(BA)D^0_m(A)T^{AB}_{\text{eff},\,ml}(\mathbf{k})\} = D^0_m(A)\delta_{mn}, \\ &\sum_l \{D^{ln}_{\mathbf{k}}(BA)[\delta_{ml} - 2D^0_m(B)T^{BB}_{\text{eff},\,ml}(\mathbf{k},\sigma)] \\ &- 2D^{ln}_{\mathbf{k}}(AA)D^0_m(B)T^{BA}_{\text{eff},\,ml}(\mathbf{k})\} = 0. \end{aligned} \quad (20)$$

Another couple of equations is obtained upon substitution $A \longleftrightarrow B$. In the matrix form, system (20) is written simply as $\hat{D}_{\mathbf{k}} = \hat{A}^{-1}(\mathbf{k})\hat{D}^0$, where

$$\hat{A}(\mathbf{k}) = \begin{pmatrix} 1 - \hat{D}^0(A)2\hat{T}^{AA}_{\text{eff}}(\mathbf{k},\sigma) & -\hat{D}^0(A)2\hat{T}^{AB}_{\text{eff}}(\mathbf{k},\sigma) \\ -\hat{D}^0(B)2\hat{T}^{BA}_{\text{eff}}(\mathbf{k},\sigma) & 1 - \hat{D}^0(B)2\hat{T}^{BB}_{\text{eff}}(\mathbf{k},\sigma) \end{pmatrix}, \quad (21)$$

$$\hat{D}^0 = \begin{pmatrix} \hat{D}^0(A) & 0 \\ 0 & \hat{D}^0(B) \end{pmatrix}.$$

Thus, the dispersion relations for quasiparticles are determined by the equation for poles of the matrix Green function $\hat{D}_{\mathbf{k}}$:

$$\left\|(E - \Omega^G_m)\delta_{mn} - 2F^G(m)T^{PG}_{\text{eff},\,mn}(\mathbf{k},\sigma)\right\| = 0. \quad (22)$$

Special features of this equation are determined by the hopping matrix $T^{PG}_{\text{eff},\,mn}(\mathbf{k},\sigma)$ and by the set of root vectors $\boldsymbol{\alpha}_m$. The local quasiparticle excitations are characterized by the energies Ω^G_m and the spectral weights $F^G(m)$ calculated as a result of the exact diagonalization of the intracell part of the Hamiltonian with allowance for strong electron correlations. In the (*A*-type) AFM phase, which exhibits FM ordering in the *xy* planes and AFM ordering between these planes along the *z* axis (Fig. 1), each orbitally ordered sublattice consists of two magnetic sublattices. This situation corresponds to four types of operators (rather than two) in Eqs. (13), implies the use of another pair of indices *G*' and *P*' in Eqs. (19), and leads to doubling of the dimension of matrix (22).

5. RESULTS OF NUMERICAL SOLUTION OF THE DISPERSION EQUATION

Figure 3a shows the results of numerical solution of dispersion equation (22) for the AFM phase. In order to

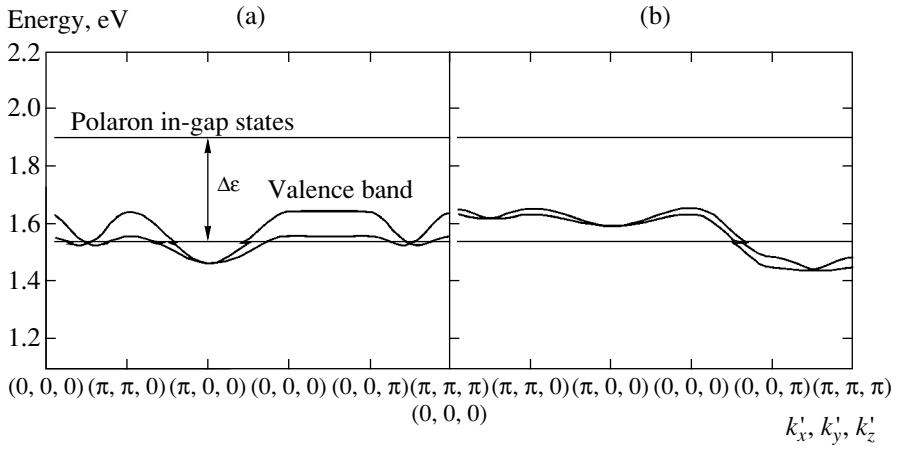

Fig. 3. Dispersion of quasiparticle states in an orbitally ordered undoped $LaMnO_3$ (a) in the state of AFM ordering and (b) in the PM phase. In order to simplify drawing, the empty states occurring in the conduction band above the gap ($E_g \geq 2$ eV) are omitted.

simplify drawing, we omitted the empty states occurring in the conduction band above the gap ($E_g \geq 2$ eV), which is formed predominantly due to the excitations with charge transfer. A numerical solution was obtained for the following parameters:

$$\varepsilon_{d_x} = \varepsilon_{d_{3y}} = 0, \quad \varepsilon_p = -2 \text{ eV}, \quad t_{pd} = 0.7 \text{ eV},$$
$$t_{pp} = 0.3 \text{ eV}, \quad U_d = 5 \text{ eV}, \quad U_p = 2 \text{ eV}, \quad (23)$$
$$J_d = 2 \text{ eV}, \quad V_{pd} = 1 \text{ eV}.$$

In selecting the ε_{d_x} and $\varepsilon_{d_{3y}}$ values, we proceeded from the fact that the presence of a crystal field does not lead to significant splitting of the e_g states [13]. In the series of electronegativity of elements, manganese (1.6) occupies a position on the left from copper (1.75). For this reason, the energy ε_p of oxygen orbitals is taken lower than that in cuprates ($\varepsilon_p \sim -1.4\ldots-1.6$ eV [11]). Since the effective radius of the Mn^{3+} ion is smaller than that of Cu^{3+} and the Mn–O bond length (1.91–2.18 Å) is greater than Cu–O (~1.89 Å), the t_{pd} and t_{pp} values in this calculation were also taken lower than in [11]. The Coulomb interaction parameters were selected so as to correspond to the calculated value (~2 eV) of the insulating gap and the experimental values reported for $LaMnO_3$.

It should be noted that the orbital ordering plays an important role in the formation of an insulating ground state in $LaMnO_3$. For comparison, we also calculated the energy band structure of cubic $LaMnO_3$ and obtained the metal ground state. Thus, at least one of the reasons for $LaMnO_3$ being an insulator is the presence of Jahn–Teller distortions and orbital ordering in the spatial structure of this manganite crystal.

Another noteworthy result is the existence of two different subbands separated by an energy interval of 0.2–0.5 eV on top of the valence band. The first subband in fact falls within the insulating gap and has nonzero dispersion at a zero spectral weight in the undoped material. At first glance, it might appear that this subband is related (by analogy with cuprates [11]) to the AFM ordering. However, the results obtained for the PM phase (Fig. 3b) do not confirm this assumption, since the band of in-gap states is retained. The origin of these states is different from that in cuprates, being related to the proximity of two orbital singlets (^5a and ^5b) in a one-hole sector of the configuration space of the system (i.e., with the distorted three-dimensional cubic structure in $LaMnO_3$). This mechanism of the formation of in-gap states was originally proposed in [23]. Emphasizing a difference in the nature of these states, we suggest calling them polaron in-gap states, since their appearance is related to the Jahn–Teller splitting of the initial orbital doublet, whereas in cuprates such states are related to the spin–polaron effect (spin-polaron in-gap states) [24].

The second subband has a nonzero dispersion and spectral density and is completely filled in the undoped manganite, thus representing a valence band. This band, in turn, consists of two close-lying bands belonging to different orbital sublattices. The bandwidth depends on the type of magnetic phase in which the given sublattice occurs (Fig. 3b). As the temperature grows above critical (T_N), the dispersion in the xy plane decreases while that in the z direction increases (which is consistent with the A-type AFM ordering). As expected, the spectra of quasiparticles are symmetric for both spin projections in the AFM and PM phases.

Figure 4 shows the results for an FM phase, which is realized in doped $La_{1-x}Sr_xMnO_3$ manganites. In this case, a partial filling (~x) of the two-hole term $|2h_{1M_{3/2}}\rangle$ takes place, and the quasiparticles corresponding to the polaron in-gap states (indicated by dashed lines in Fig. 2) exhibit dispersion and acquire a nonzero spec-

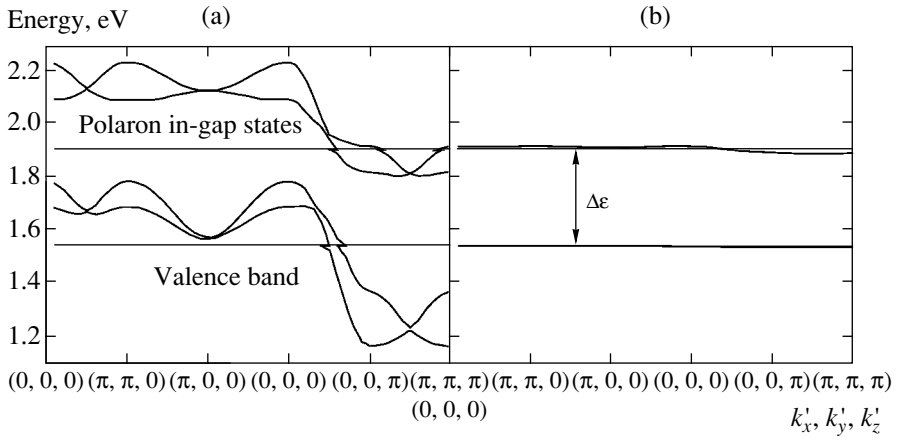

Fig. 4. Dispersion of quasiparticle states in an orbitally ordered doped $La_{1-x}Sr_xMnO_3$ manganite in the state of FM ordering (x = 0.3) for the charge carrier spin (a) $\sigma = \uparrow$ and (b) $\sigma = \downarrow$.

tral weight ~x. The FM ordering removes the degeneracy with respect to spin, and an increase in x leads to the formation of a state with an insulating gap for one spin subband and with a metallic character for the other subband. Such states are referred to as half-metallic (see, e.g., review [25]). Above the Curie point, the bands in the PM phase exhibit narrowing and a gap opens in the quasiparticle spectrum of the half-metallic phase. Detailed consideration of the mechanism of colossal magnetoresistance goes beyond the scope of this paper and will be presented in a separate publication.

6. CONCLUSIONS

The generalized tight binding method was developed for calculations of the electron band structure in Mott–Hubbard insulators, that is, in the regime of strong electron correlations, where the traditional one-electron schemes such as LDA are inapplicable. The first class of strongly correlated systems for which calculations within the framework of the generalized tight binding method were performed were cuprates [11]. It was established that the band structure of quasiparticles strongly depend on the doping level, the temperature, and other external factors. In particular, in-gap states can appear with small a spectral weight proportional to the dopant concentration.

The results obtained in this study showed that the generalized tight binding method is also applicable to systems with high-spin many-electron terms. The most important specific property of manganites is the orbital ordering that removes degeneracy of the ${}^5e_g$ doublet. Without this removal of degeneracy, the band structure of $LaMnO_3$ would be metallic despite strong electron correlations and AFM ordering. The physics of this conclusion is quite simple: a degenerate ${}^5e_g$ doublet corresponds to a two-band Hubbard model with 1/4 filling of each band and, hence, splitting of the one-electron band into two Hubbard bands retains the metallic state.

ACKNOWLEDGMENTS

This study was supported in part by the Interdisciplinary Integration Project of the Siberian and Ural Divisions of the Russian Academy of Sciences (project no. 74), the "Quantum Macrophysics" Program of the Presidium of the Russian Academy of Sciences, and the Russian Foundation for Basic Research (project no. 06-02-16100).

REFERENCES

1. C. Zener, Phys. Rev. **82**, 403 (1951).
2. P. W. Anderson and Hasegawa, Phys. Rev. **100**, 675 (1955).
3. P. G. de Gennes, Phys. Rev. **118**, 141 (1960).
4. Yu. A. Izyumov and Yu. N. Skryabin, Usp. Fiz. Nauk **171**, 121 (2001) [Phys. Usp. **44**, 109 (2001)].
5. N. G. Bebenin, R. Zainulina, V. V. Mashkaustan, et al., Phys. Rev. B **69**, 104434 (2004).
6. Y.-D. Chuang, A. D. Gromko, D. S. Dessau, et al., Science **292**, 1509 (2001); T. Saitoh, D. S. Dessau, Y. Marimoto, et al., Phys. Rev. B **62**, 1039 (2000).
7. D. S. Dessau and Z.-X. Shen, in *Colossal Magnetoresistive Oxides,* Ed. by Y. Tokura (Gordon and Breach, Amsterdam, 1998), p. 1.
8. J. Zaanen, G. A. Sawatzky, and J. W. Allen, Phys. Rev. Lett. **55**, 418 (1985).
9. W. E. Pickett and D. Singh, Phys. Rev. B **53**, 1146 (1996).
10. W. E. Pickett, H. Krakauer, R. E. Cohen, and D. Singh, Physica C (Amsterdam) **162–164**, 1419 (1989).
11. V. A. Gavrichkov, S. G. Ovchinnikov, A. A. Borisov, and E. G. Goryachev, Zh. Éksp. Teor. Fiz. **118**, 422 (2000) [JETP **91**, 369 (2000)].

12. K. I. Kugel' and D. I. Khomskiĭ, Zh. Éksp. Teor. Fiz. **64**, 1429 (1973) [JETP **37**, 725 (1973)]; Usp. Fiz. Nauk **136**, 621 (1982) [Sov. Phys. Usp. **25**, 231 (1982)].
13. A. J. Millis, in *Review Notes in Summer College and Conference on Physics and Chemistry of Rare-Earth Manganites* (ICTP, Trieste, 2003), SMR1505/33.
14. J. Hubbard, Proc. R. Soc. London, Ser. A **276**, 238 (1963).
15. R. O. Zaĭtsev, *Diagram Methods in the Theory of Superconductivity and Ferromagnetism* (Editorial URSS, Moscow, 2004) [in Russian].
16. V. V. Val'kov and S. G. Ovchinnikov, *Quasi-particles in Strongly Correlated Systems* (Sib. Otd. Ross. Akad. Nauk, Novosibirsk, 2001) [in Russian].
17. I. V. Solovyev and K. Terakura, J. Korean Phys. Soc. **33**, 375 (1998).
18. W. Koshibae and S. Maekawa, Physica C (Amsterdam) **317–318**, 205 (1999).
19. X.-J. Fan, S.-Q. Shen, Z. D. Wang, et al., Phys. Rev. B **62**, 3869 (2000).
20. T. Hotta, A. L. Malvezzi, and E. Dagotto, Phys. Rev. B **62**, 9432 (2000).
21. S. M. Dunaevskiĭ, Fiz. Tverd. Tela (St. Petersburg) **43**, 2161 (2001) [Phys. Solid State **43**, 2257 (2001)].
22. R. O. Zaĭtsev, Zh. Éksp. Teor. Fiz. **68**, 207 (1975) [Sov. Phys. JETP **41**, 100 (1975)].
23. S. G. Ovchinnikov, Zh. Éksp. Teor. Fiz. **102**, 534 (1992) [Sov. Phys. JETP **75**, 283 (1992)].
24. S. G. Ovchinnikov, A. A. Borisov, V. A. Gavrichkov, and M. M. Korshunov, J. Phys.: Condens. Matter **16**, L93 (2004).
25. V. Yu. Irkhin and M. I. Katsnelson, Usp. Fiz. Nauk **164**, 705 (1994) [Phys. Usp. **37**, 659 (1994)].

Translated by P. Pozdeev